New Concept of Space Radiator with Variable Emittance

Valeri V. Vlassov
vlassov@dem.inpe.br
National Institute for Space Research – INPE

Fabiano Luis de Sousa
fabiano@dem.inpe.br
National Institute for Space Research – INPE

Ana Paula C. Cuco
apcuco@gmail.com
National Institute for Space Research – INPE

Antônio J. Silva Neto
ajsneto@iprj.uerj.br
Polytechnic Institute
State University of Rio de Janeiro – IPRJ/UERJ

A new concept of space radiator of variable emittance for satellite thermal control is presented. The radiator is composed of two stages which exchange heat through radiation between finned surfaces covered with variable emittance coatings, whose emissivity is increased with temperature. Under cold conditions the radiative heat coupling between the stages is minimal, preventing the equipment subcooling, while in hot conditions the heat exchange is increased. A steady-state mathematical model was developed and numerically coupled to an optimization algorithm, and a design optimization procedure was performed. Two optimization criteria were employed: minimization of the radiator mass and the power consumption of heater under cold conditions. The Generalized Extremal Optimization algorithm was used as the optimization tool. The design was then modeled in detail using the SINDA/Fluint package considering orbital conditions of the EQUARS satellite. The performance of the radiator concept proposed here was also compared to a conventional design, for the same operational conditions. It is envisioned that the utilization of such radiators in micro-satellites will lead to considerable electric power savings for safe heaters and may contribute to a longer satellite life. In the design trade-off, the cost for this saving is additional radiator mass and volume.
Keywords*: space radiator, variable emittance coating, optimal design, mathematical model, Generalized Extremal Optimization*

Introduction

The temperature of satellite components (equipment, structure elements, etc) is defined completely by the equilibrium between internal heat dissipation and external heat fluxes. For non-dissipating external components exposed to Space, such as Multi-Layer Insulation blankets (MLIs) and antennas, their temperatures may vary in the range from about -150^{o}C up to +150^{o}C. However, for the electronic equipment and structure, the temperatures must be maintained within a range typically from -10 to +40^{o}C. (Gilmore, 2002) A common design approach in satellite thermal control is to thermally insulate most of its external surfaces, while allowing certain areas (radiate windows or radiators) to reject heat to Space. The usual method in designing the radiator is to size it to accommodate a combination of maximum internal heat loads and external fluxes, defined as the Hot Case (HC). Then, it is verified if this radiator area can also accommodate the Cold Case (CC), when the satellite is subjected to the lowest external heat flux and reduced equipment dissipation. If a radiator size leads to a temperature in the equipment, during the CC, below its minimum required limit, heaters are usually used to warm up the equipment. Although being a simple and efficient solution to overcome low temperatures in the Cold Case, heaters consume electrical power, which is a limited resource in any spacecraft. In fact, they can consume from 10 to 40% of the total electrical power budget when the satellite is in cold conditions.

When the power budget is limited, other types of thermal control devices instead of heaters can be used in order to cope with the CC low temperatures, such as thermal louvers (Karan, 1998; Parisoto et al., 1996, Muraoka et al., 2001) or a radiator with variable conductance heat pipes (Fleischman et al., 1978,). These devices save power consumption, but add mass and increase the complexity of the thermal control subsystem. Hence, there is a trade-off between power consumption and mass, as well as reliability that must be taken into account when selecting a thermal control device for a given satellite.

Recently, a new solid state technology that changes its surface emmitance as a function of temperature was developed (Tachikawa et al., 2000, 2001 and 2003; Shimakawa et al., 2002). The prototype is a ceramic thin plate, which uses the feature of the ferromagnetic metal-insulator transition effect that increases the emissivity with temperature rising. The effective emmitance variation of these devices is of the same order of the effective emittances obtained in radiators with thermal louvers, but it has the advantage of having no moving parts. On the other hand, they present a high absorptivity (above 0.80), what is an undesirable characteristic for any radiator because of effectiveness degradation when exposed to the Sun flux.

In order to avoid the problem with the high absorptivity of the variable emissivity coating, a new concept for a space radiator was proposed (Vlassov et al., 2006b). Called VESPAR (Variable Emmitance SPAce Radiator), it takes the advantage of the variable emissivity, while keeping a low absorptivity for the entire assembly. The VESPAR is composed of two stages having internal extended fin surfaces for improving radiative heat transfer between them.

The feasibility of the proposed concept was verified by numerical simulations using a simplified mathematical model describing the radiator operating in steady-state conditions (Vlassov et al., 2006b). This model was coupled to an optimization algorithm and a design optimization procedure performed. Two optimization criteria were employed: minimization of the radiator mass and also the power consumption of heaters. The dimensions of the radiator were the design variables. The performance of VESPAR was compared to a traditional design for the same operational conditions and the results showed that it may lead to a significant reduction on demand for heater power during the CC. The Generalized Extremal Optimization (GEO) (de Sousa et al., 2003) was used as the optimization algorithm. GEO is a recently proposed evolutionary algorithm devised to be applied to complex optimization problems and has been used successfully in aerospace applications.

In this paper the thermal performance of the VESPAR concept is further investigated. Based on the optimal geometry found for the radiator, a detailed numerical model was built using the SINDA/FLUINT/Thermal Desktop thermal analysis software and numerical simulations performed for a planned space mission, the EQUARS satellite (Fonseca et al., 2004). The results of this detailed modeling confirmed the gain in satellite power saving when using VESPAR. The procedure used for the proof-of-concept of VESPAR is revised, the radiator's mathematical model is presented, and

Paper accepted March, 2010. Technical Editor: Eduardo Belo.

results for VESPAR performance on EQUARS mission are compared to a traditional radiator design.

Nomenclature

A = *Area, m^2*
B = *Width, m*
G = *Thermal conductance, W/K*
H = *Height of radiator fins, m*
k = *Thermal conductivity, W/K·m*
L = *Length, m*
M = *Mass, kg*
N = *Number of fins in radiator bottom plate*
Q = *Heat load, W*
Q = *Heat flux, W/m^2*
T = *Temperature, K*
w = *Distance between fins of each plate, m*
V = *Volume, m^3*

Greek Symbols

α = *Solar absorptivity*
δ = *Thickness, m*
ε = *Emissivity*
γ = *Mass per area unit, kg/m^2*
η = *Effectiveness*
φ = *Power requirement*
λ = *Relative importance criteria factor*
ρ = *Density, kg/m^3*
σ = *Stefan-Boltzmann constant, $W/m^2 \cdot K^4$*
$\chi(.)$ = *Heaviside step function*

Subscripts

A Area
eff Effective
eq Equipment
f Fin
h Heater
IR Infrared
m Mass
r Radiator
s Solar
w Wall
v Variable emittance
0 Conventional radiator
1 Internal stage
12 Between two stages
2 External stage

VESPAR Design Concept

The proposed radiator consists of two similar finned parts (stages) as shown in Fig. 1. The stages are assembled in such a way that direct thermal contact by conduction is avoided or minimized by the use of insulation washers, and they exchange heat primarily by radiation. The internal radiator part receives heat dissipated from equipment through conduction, then, the heat is transferred to the external stage by radiation through the finned surfaces, and is rejected to space by the external surface of the upper stage. While the external radiator part has its outer surface covered with a solar-reflective coating, as is usual to conventional space radiators (Gilmore, 2002), the internal finned surfaces are covered with a variable emissivity material whose emissivity is increased as its temperature increases. Therefore, under cold conditions the radiative heat link between these surfaces is minimal, keeping a greater fraction of the equipment dissipated heat for its own warming. By such way the temperature of the equipment is prevented from decreasing too much. On the other hand, during hot conditions, the thermal coupling is increased between the variable emittance surfaces and a great fraction of the equipment dissipated heat is transferred to the external stage and then rejected to space. By such way the temperature of the equipment is kept below its maximum limit.

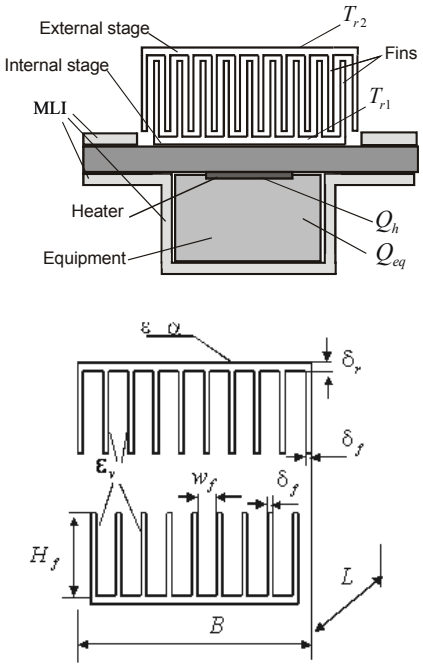

Figure 1. Two stage radiator assembly.

With such a two-stage concept, the intrinsic high solar absorptivity of the variable emittance coating is not an issue anymore: the Sun heat flux does not enter the interior of the radiator, and the external surface of the upper stage is covered with a conventional solar reflector coating, with low absorptivity. Moreover, with the use of VESPAR there is an increase on the area available to radiate heat to space. In the HC, this increases the ability of the radiator to reject heat to space.

Analytical Thermal Model for Optimal Design

In order to verify the efficiency of the proposed radiator concept and obtain the optimal design parameters, it was considered an application where the radiator is mounted on the outer side of a satellite structural panel, and the equipment box is installed on the internal side of the panel, as shown in Fig. 1. They are thermally coupled through the panel. All surfaces but the radiator are covered with multilayer insulation blankets (MLIs), and a heater is attached to the equipment. Such configuration is typical for 3-axis stabilized micro satellites, like the Brazilian Equars or SSR1 (Kono et al., 2003), and also similar to the one adopted for the thermal control of the battery compartment of the China-Brazil Earth Resources Satellite (Lino et al., 2000).

For the definition of the main dimensions of radiator elements through an optimal design approach, a computationally inexpensive analytical heat transfer model of the system was adopted and integrated to the optimization tool. The main assumptions used in the model were:

- The radiator operates in steady state mode.
- The radiator base plate is a square ($L = B$, see Fig. 1).

- The heat conduction in the panel's XY plane is neglected.
- Lateral surfaces of the external stage, which are situated perpendicular to the fins, are not considered in the internal radiative heat transfer (conservative approach).
- Conductive heat leak from the upper stage to the panel through elements of fixation is neglected.
- Temperature distributions over the internal fins are accounted through effectiveness coefficients and average temperatures.

For the hot case the heat transfer from the equipment to the radiator internal stage is described by

$$Q_{eq,max} = G_{eq}(T_{eq,max} - T_{r1,max}) \tag{1}$$

Heat transfer from the radiator internal stage to the external one is given by

$$Q_{eq,max} = \varepsilon_{12}(T_{r1,max}, T_{r2,max}) A_{12} \sigma (T_{r1,max}^4 - T_{r2,max}^4) \tag{2}$$

The heat exchange between the external radiator surface and the outer environment is given by

$$Q_{eq,max} = (L^2 + 2\eta_{f2} LH_f)\left(\varepsilon\sigma T_{r2,max}^4 - \alpha q_{s\,max} - \varepsilon q_{IR\,max}\right) \tag{3}$$

where η_{f2} accounts for the fin effect due to the lateral edges of the radiator's second stage, whose expression will be introduced later in the text.

The unknown temperatures of the radiator for the hot case $\{T_{eq,\max}, T_{r1,\max}, T_{r2,\max}\}$ are obtained by numerically solving the set of equations 1-3 using the secant method.

For cold conditions, the heater dissipation is added to the equilibrium equations:

$$Q_{eq,min} + Q_h = G_{eq}(T_{eq,min} - T_{r1,min}) \tag{4}$$

$$Q_{eq,min} + Q_h = \varepsilon_{12}(T_{r1,min}, T_{r2,min}) A_{12} \sigma (T_{r1,min}^4 - T_{r2,min}^4) \tag{5}$$

$$Q_{eq,min} + Q_h = (L^2 + 2\eta_{f2} LH_f)\left(\varepsilon\sigma T_{r2,min}^4 - \alpha q_{s\,min} - \varepsilon q_{IR\,min}\right) \tag{6}$$

Equations (4)-(6) are first solved for unknowns $\{T_{eq,min}, T_{r1,min}, T_{r2,min}\}$, having $Q_h = 0$. If the obtained minimal temperature of equipment has dropped below the allowable low limit, i.e., $T_{eq,min} < T_{min}$, it means that extra heating is needed and the heater should be turned on. To obtain the power needed to keep the equipment temperature above its low limit, in Eq. (4), the equipment temperature is fixed on this limit, $T_{eq,min} = T_{min}$, and equations 4-6 are solved again, this time for unknowns $\{Q_h, T_{r1,min}, T_{r2,min}\}$.

The total average effective area of radiative heat transfer between the radiator stages can be expressed as

$$A_{12} = (L - (2N_f + 1)\delta_f)L + N_f \eta_{f1} H_f L + N_f \eta_{f2} H_f L \tag{7}$$

Here N_f is the number of fins on the internal stage (bottom plate in Fig. 1). The effective emissivity inside each individual enclosure can be approximately evaluated by the relationship for radiative heat transfer between two gray plates, each of them with homogeneous temperature (Isachenko and Sukomel, 2000):

$$\varepsilon_{12}(T_{r1}, T_{r2}) = \frac{1}{\frac{1}{\varepsilon_v(T_{r1})} + \frac{1}{\varepsilon_v(T_{r2})} - 1} \tag{8}$$

The fins efficiency is expressed by the analytical solutions of heat conduction problem for a fin with radiative heat transfer boundaries (Isachenko and Sukomel, 2000).

$$\eta_{fi} = \frac{tanh(r_i H_f)}{r_i H_f}; \qquad r_i = \sqrt{\frac{8\varepsilon_v(T_{ri})\sigma T_{ri}^3}{k\delta_f}} \tag{9}$$

The internal surfaces of the radiator are covered with the coating of variable emissivity, having the temperature-dependent performance curve, as presented by Tachikawa et al. (2000). The emissivity as a function of temperature has been approximated by the Boltzmann model in the temperature range 150-350 K:

$$\varepsilon_v(T) = \varepsilon_2 - \frac{\varepsilon_2 - \varepsilon_1}{1 - e^{\frac{T - T_0}{\Delta T}}} \tag{10}$$

The best curve fitting parameters are $\varepsilon_1 = 0.24052$, $\varepsilon_2 = 0.62165$, $T_0 = 261.10302$ K, $\Delta T = 18.29369$ K.

The mass of the radiator is obtained by

$$M_t = \rho\left(L^2\delta_r + N_f LH_f \delta_f\right) + \rho\left(L^2\delta_r + 2LH_f\delta_f + (N_f - 1)LH_f\delta_f\right) + \gamma_A A_{12} \tag{11}$$

The last term in Eq. (11) is the total mass of the variable emittance coating, which depends on the total surface area involved in the internal radiative heat transfer.

For comparison purposes, a conventional radiator is dimensioned for the same assembly configuration and operation conditions imposed to the two-stage radiator proposed here. The conventional radiator is a square flat plate of length L_0 and with the same thickness δ_r of the VESPAR base plate. Its coating is the same as the one in the outer surface of the two-stage radiator. The length L_0 of the conventional radiator is determined from the requirement to keep the equipment temperature within its operational range. Hence, a heater is also turned on if the equipment temperature falls below the lower limit ($T_{\min}$), dissipating Q_{h0}.

The minimum heater power Q_{h0} of the conventional radiator, necessary to drive up the equipment temperature to a level above the minimum value required ($T_{\min}$) can be obtained by solving the following equations with respect to the unknowns $\{Q_{h0}, T_{r0,\min}\}$:

$$Q_{eq,min} + Q_{h0} = G_{eq}(T_{min} - T_{r0,min}) \tag{12}$$

$$Q_{eq,min} + Q_{h0} = L_0^2\left(\varepsilon\sigma T_{r0,min}^4 - \alpha q_{s\,min} - \varepsilon q_{IR\,min}\right) \tag{13}$$

The total mass of the conventional radiator is given by

$$M_{t0} = \rho\left(L_0^2 \delta_r\right) \tag{14}$$

The values Q_{h0} and M_{t0} are used in the definition of the optimization criteria. More details on the model can be found in (Vlassov et al., 2006b).

Algorithm Optimization Criteria, Design Variables and Fixed Parameters

A recently developed global search evolutionary algorithm, called Generalized Extremal Optimization (GEO), is used as the optimization tool. The GEO algorithm was developed to be applied to complex optimization problems. It is based on the Extremal Optimization (EO) method proposed by Boettcher and Percus (2001) that was inspired by the simplified evolutionary model of Bak and Sneppen (1993). Belonging to the general class of stochastic methods, GEO can deal with any kind of design variables either continuous, integer, discrete or a combination of them. Not depending on derivatives of the objective function or constraints, it can be applied to highly nonlinear problems that present a multimodal, or even disjoint, design space. In GEO a string of bits encodes the design variables. Being an evolutionary algorithm, each bit is considered a species and has an associated fitness. This number depends on the adaptability of the bit, that in GEO is related to the improvement or not, on the value of the objective function if the bit is flipped (from one to zero or vice-versa). GEO has been applied successfully to real complex design problems, including heat pipe design (Vlassov et al., 2006a). It has also proven to be competitive in comparison to other popular stochastic algorithms such as Genetic Algorithm and Simulating Annealing, with the a priori advantage of having only one free parameter to tune. The algorithm is described in detail in (de Sousa et al., 2003).

The design of the radiator is formulated as an optimization problem:

$$\text{Minimize: } f\{M_t, Q_h\} \tag{15}$$

Subject to:

$$x_{min} \le x \le x_{max} \quad \text{and} \quad T_{min} \le T_{eq} \le T_{max} \tag{16}$$

where **x** is the vector of design variables and T_{eq} is the equipment temperature. The design variables, with the respective feasible ranges are presented in Table 1. The temperature of the equipment must lie in the range [-10, +40] ^{o}C, which is the temperature range usually used as requirement for operation of general electronic equipment in satellites.

For the present analysis the multi-objective problem (minimization of heater power and radiator mass) was transformed into a mono-objective problem by the weight penalty method (Vanderplaats, 1998), and the objective function then defined as:

$$f_o = \lambda_m \frac{M_t}{M_{t0}} + \lambda_h \frac{Q_h}{Q_{h0}} \qquad \lambda_m + \lambda_h = 1 \tag{17}$$

The objective function was normalized by the mass and power of the conventional radiator. Ideally, the mass of the proposed radiator would match the mass of the conventional one, whereas its heater dissipation would come to zero, that is:

$$\frac{M_t}{M_{t0}} \to 1; \qquad \frac{Q_h}{Q_{h0}} \to 0$$

The optimization variables are the dimensions of the base plate, and the dimensions and number of fins.

The design variables are summarized in Table 1. The number of bits used to encode each design variable is defined by its desired resolution. In the last two columns of Table 1 the number of bits and the associated resolution of each design variable are presented.

Results of Optimization

Figure 2 shows the sets of near-optimal solutions, plotted as a function of the best values found for one of the geometrical design variables, the radiator fin height.

The radiator design optimization took 400 independent runs of GEO. Each run was stopped after 10^6 function evaluations. In the small box inside Fig. 2, the sets are plotted in a scale that shows the bound constraints for the geometric design variables.

In Table 3 the four best solutions obtained for VESPAR from the set of results are presented, along with the design parameters calculated for the conventional radiator.

The fixed parameters used in the design optimization are described in Table 2.

Table 1. Design variables.

Variable	Feasible Range	Type	Description	Number of bits	Resolution
L	[0.3, 0.5] m	Continuous	Length of radiator	6	5 mm
H_f	[0.02, 0. 16] m	Continuous	Height of fins	9	0.5 mm
δ_f	[0.1, 1.5] mm	Continuous	Thickness of fin	6	0.025 mm
N_f	[1, 32]	Integer	Number of fins	5	1
Q_h	[0, 15] W	Continuous	Heater Power	8	0.1 W

Table 2. Fixed parameters.

Parameter	Value	Description
T_{min}	-10 ^{o}C	Minimum allowable temperature of equipment
T_{max}	+40C	Maximum allowable temperature of equipment
$Q_{eq,min}$	5W	Minimal dissipation of equipment
$Q_{eq,max}$	25W	Maximal dissipation of equipment
q_{max}	201	Absorbed external heat flux at hot case
q_{min}	33.5	Absorbed external heat flux at cold case
δr	2.0 mm	Thickness of base plate
w_{min}	1 mm	Limit on minimal space between fins
δ_ε	0.1mm	Thickness of variable emissivity coating
γ_A	0.85 kg/m^2	Areal mass of the variable emissivity coating
G_{eq}	10 W/K	Thermal conductance of the equipment interface
k	120 W/(K·m)	Thermal conductivity of radiator material (Al)
ρ	2768 kg/m^3	Density of radiator material

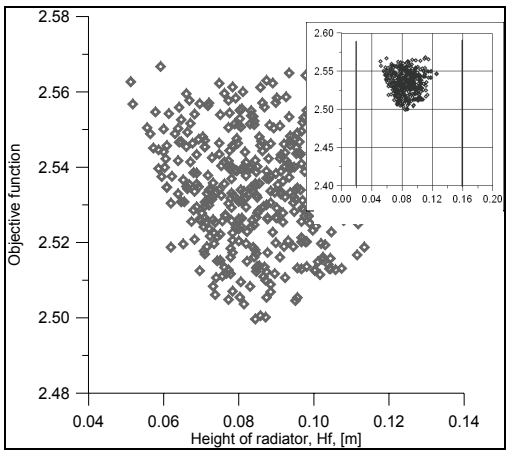

Figure 2. Mapping of near-optimal solutions, plotted as a function of the radiator fin height, H_f.

From Table 3 it can be seen that only around half of the heater power used in the conventional assembly is necessary for VESPAR, operating with the same boundary conditions. The penalty in mass was around 2 kg. It can also be seen that the radiator area of VESPAR is almost the same as the area of the conventional one, so there will be no impact on the area of the satellite covered by the radiator, by using VESPAR. These results indicate that the VESPAR concept can be a very attractive option for satellites with limited availability of electrical power.

All results shown here were obtained using equal weighting factors ($\lambda_m = \lambda_h = 0.5$) in the definition of the objective function, i.e., it was given the same importance for each optimization criterion. Full domain of Pareto-optimal solutions can be obtained by the performing of multiple solutions through variation of the weighting factors within ~0.05...0.95, keeping the condition of normalization, given in Eq. (17) (Messac et al., 2000).

Table 3. Best design parameters found for VESPAR and the conventional radiator.

Type of Radiator	Objective Function, Eq. (17)	Q_h [W]	M_t [kg]	L [m]	H_f [mm]	δ_f [mm]	N_f
VESPAR	2.499	7	2.551	0.344	84.38	0.478	5
	2.500	7.29	2.541	0.347	87.12	0.389	5
	2.500	7.17	2.546	0.347	85.75	0.411	5
	2.503	7.52	2.536	0.338	81.37	0.389	6
Conventional radiator	-	15.00	0.560	0.320	-	-	-

FEM Model

Based on the results obtained with the design optimization procedure, a detailed numerical model of VESPAR assembled in a satellite panel was developed using the SINDA-FLUINT Thermal DeskTop Analyzer (Panczak et al., 2005). The model comprises the radiator, the satellite panel and an equipment box, as shown in Fig. 3.

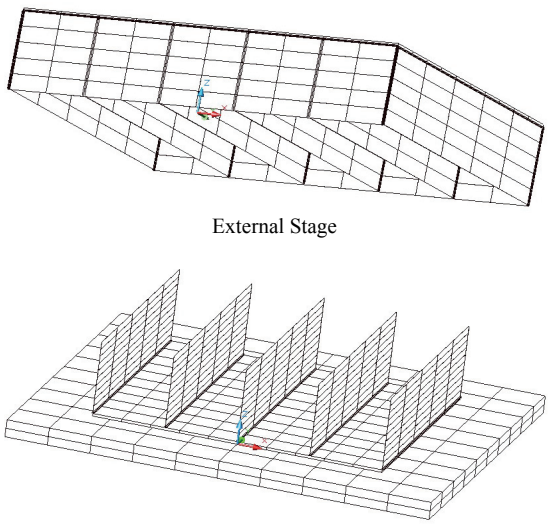

External Stage

Internal Stage

Figure 3. FEM VESPAR nodal breakdown; base plate and internal stage below, and second stage above.

The dimensions of the radiator used in the detailed model were based on the best solutions found in the conceptual design procedure. From Table 3 it was chosen the solution with minimal heater power consumption. Hence, the dimensions for the radiator used in the detailed model were: a) the internal stage has 5 fins of 84 mm in height and 0.46 mm in thickness each, and its base plate has a footprint of 0.344 x 0.344 m and 3 mm thickness; b) the external stage has 4 internal fins of the same dimension and 4 lateral fins of 2 mm in thickness; the top plate has a footprint of 0.43 x 0.356 m. The external surface area of VESPAR, available for radiation to Space is 2.41 times larger than the conventional radiator area. In the analysis the radiator was considered to be made of Al 2024.

In detailed VESPAR FEM numerical model, each fin is represented by 25 isothermal elements, the baseplate by 100 elements and the satellite panel by 200 elements. The radiative couplings between two given elements are calculated by ThermalDesktop using a Monte-Carlo ray-tracing technique and the conductive couplings are generated using the finite element method.

As in the conceptual study presented before, for comparative purpose, a detailed numerical model of a conventional radiator was also built. Views of the nodal breakdown for VESPAR and the conventional radiator are shown in Fig. 4.

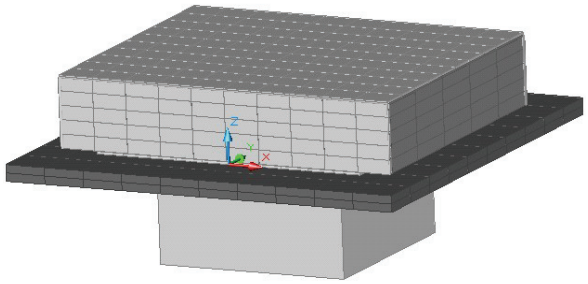

VESPAR

Figure 4. View on VESPAR (above) and a corresponding conventional radiator (below).

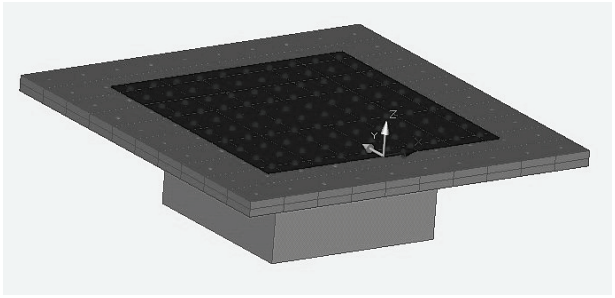

Conventional

Figure 4. (Continued).

The outer surface of VESPAR second stage and the conventional radiator surface are covered with an Optical Surface Reflector (OSR) coating. Both radiators are positioned over a honeycomb panel with dimensions 0.5 x 0.5 x 0.02 (m). The thermal contact conductance of VESPAR with the panel is 1500 W/m^2K and from the panel to the equipment is 1000 W/m^2K. The equipment has a footprint of 0.24 m x 0.24 m and height of 0.12 m. The MLI covering all, but the radiator areas (see Fig. 1) has an external layer of polyimide film having 0.55 absorptivity and 0.69 emissivity at satellite End Of Life (EOL).

Modeling Results: Conventional Radiator

The performance of VESPAR and the conventional radiator are evaluated under hot and cold cases. The hot case corresponds to maximal equipment heat dissipation, maximal external heat flux and EOL conditions for the thermal coating. The cold case corresponds to minimal equipment dissipation, minimal external heat flux and Begin of Life (BOL) conditions for the thermal coating. The external heat fluxes correspond to the orbit of the scientific satellite EQUARS (Fonseca et al., 2004), which has an altitude of 750 km and inclination of 20 degrees. The external coating is OSR with $\alpha/\varepsilon = 0.12/0.81$ for BOL conditions and $\alpha/\varepsilon = 0.24/0.79$ for EOL conditions. The orbits and attitudes of the assembly, corresponding to the hot and cold cases are shown in Fig. 5. The HC attitude corresponds to the normal mode of satellite operation, when its Z+ axis is pointed to Earth (collecting data and images). The CC attitude corresponds to the so-called safe mode, when a contingency or failure occurs and the satellite enters in inertial stabilization, in which its Z- axis is pointed to the Sun together with the solar panel, in order to guarantee electric power needed for recuperation. In the safe mode many equipment dissipate minimal power or are switched-off. It is assumed that the assembly composed by the radiator and its supporting panel is thermally decoupled from the satellite.

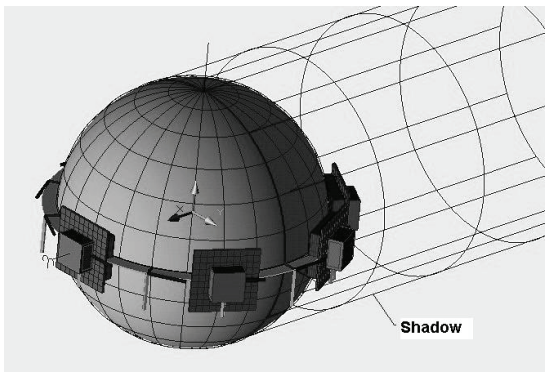

Figure 5. Hot and cold case orbits and attitudes.

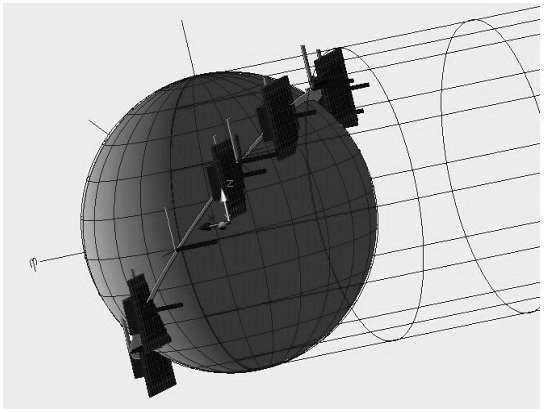

Figure 5. (Continued).

The average absorbed orbital heat fluxes for the conventional radiator, calculated with RadCAD/Thermal Desktop tool, are q_{max} = 209.8 W/m^2 and q_{min} = 50.1 W/m^2 for hot and cold case respectively.

The temperature map under orbit-average heat loads on the conventional radiator is shown in Fig. 6. The HC temperature scale is shown on the left side of the figure, and the CC one on the right side.

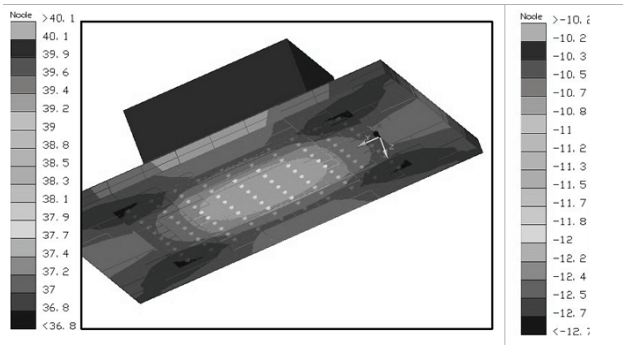

Figure 6. Temperature maps for conventional radiator assembly for hot (left temperature scale) and cold (right temperature scale) cases.

Considering the maximum equipment heat dissipation ($Q_{eq,max}$ = 25 W) during the HC, its temperature reaches + 40.1°C in steady-state conditions. The modeling results show that under the cold case conditions, in order to keep the equipment above its minimal temperature limit of -10°C, the aggregate dissipation of heater Q_h and equipment should be 19.2 W, or as much as 77% of $Q_{eq,max}$.

Modeling Results: VESPAR Radiator

For VESPAR, the temperature of the equipment reached 26.5°C in the HC, when the equipment was dissipating 25 W. This is 13.6°C less than the temperature reached by the equipment in the same thermal conditions, but using the conventional radiator. This decrease on the equipment temperature was due to the higher radiation area provided by VESPAR using the same footprint area. In fact, VESPAR could accommodate an equipment dissipation of up to 32.2 W before the equipment temperature surpasses the limit of 40°C. To accommodate the same capacity of heat rejection, the conventional radiator would need an increase of 29% on its radiative area. In Fig. 7 it is shown the temperature distribution on the fins of the internal stage of VESPAR.

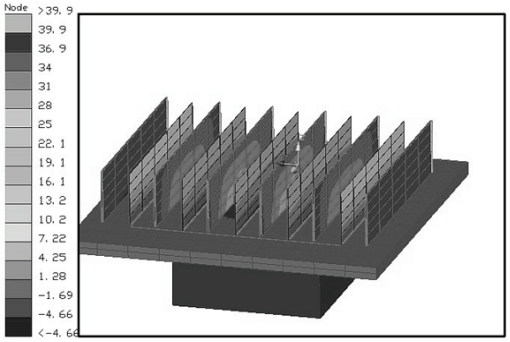

Figure 7. Steady state hot case temperature maps on elements of VESPAR radiator internal stage.

The corresponding temperature maps obtained for the cold case are shown in Fig. 8.

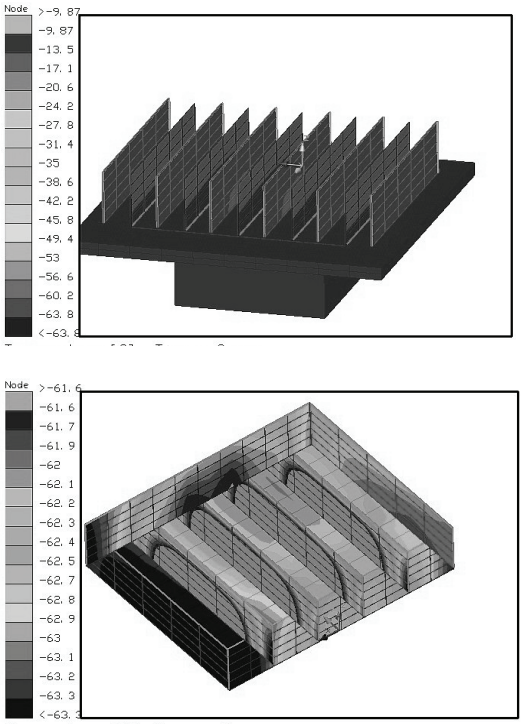

Figure 8. Steady state cold case temperature maps on the internal (above) and external (bellow) stages of VESPAR.

Under CC conditions the total power (heat load plus heaters) needed to keep the equipment above the lower limit of –10°C is 14.3 W, which is 44% of $Q_{eq,max}$. Compared to conventional radiator relative power requirement of 77% of $Q_{eq,max}$ to avoid equipment subcooling, we have 33% of aggregate power saving.

From Table 5 it can be seen clearly that the VESPAR concept provides a significant saving in heater power. The detailed analysis confirmed the results from the conceptual simplified model, even with better results. These results can be better understood and generalized with the introduction of some dimensionless performance parameters, as presented next.

First, we define a relative dimensionless amplitude for the variation of the equipment heat dissipation:

$$\Delta\overline{Q} = \frac{Q_{eq,max} - Q_{eq,min}}{Q_{eq,max}} \tag{18}$$

Second, we set in a similar way the dimensionless amplitude of variation of external absorbed fluxes in cold and hot cases

$$\Delta\overline{q} = \frac{q_{max} - q_{min}}{q_{max}} \tag{19}$$

The relative heater power needed to keep the equipment above its lower limit is defined as:

$$\overline{Q}_h = \frac{Q_h}{Q_{eq,max}} \tag{20}$$

In general, the higher the values of either $\Delta\overline{Q}$ or $\Delta\overline{q}$ or both, the higher the need for heater power.

Summary of Results

In Table 4 the physical main parameters and thermal performance for VESPAR and the conventional radiator are presented, for both the conceptual and detailed analysis.

Now we introduce a dimensionless criterion of the thermal control power requirement :

$$\varphi_h = \frac{\overline{Q}_h}{\Delta\overline{q} + \Delta\overline{Q}} \tag{21}$$

The φ_h parameter gives a relation between the need for heater power during cold conditions and the amplitude variation of external heat fluxes and equipment heat dissipation. The lesser the φ_h magnitude, the better. In the ideal case, no power is needed to keep the equipment temperature above its lower limit, i.e. $\varphi_h \to 0$. The magnitude of this characteristic depends also on the required temperature range i.e. $\Delta T = (T_{max}\text{-}T_{min})$. When $\Delta T \to 0$, then $\varphi_h \to 1$ for conventional radiators. Therefore, φ_h may vary within 0 and 1. It is also assumed that on the uncertainty 0/0, $\varphi = 0$, which means no control power is needed if external condition and equipment dissipation are constants.

We also should define relative mass and volume of VESPAR radiators with respect to saving heater power:

$$C_M = \frac{M_{VESPAR} - M_{conv}}{Q_{h,conv} - Q_{h,VESPAR}} \; ; \; C_V = \frac{V_{VESPAR} - V_{conv}}{Q_{h,conv} - Q_{h,VESPAR}} \tag{22}$$

Based on the introduced dimensionless characteristics we can now perform a generalization and comparison of the results presented before. Table 5 summarizes these characteristics for all considered radiators.

As can be seen from Table 5, the generalized characteristics for VESPAR obtained with the simplified and detailed models are very similar, what confirms the effectiveness of the use of the simplified model for the optimization and conceptual design.

Table 4. Absolute performances of radiators.

	$Q_{eq,max}$ [W]	$Q_{eq,min}$ [W]	q_{max} [W/m^2]	q_{min} [W/m^2]	Qh [W]	ΔQh, saved	LxBxH [mm]	V [liters]	M [kg]
VESPAR (Concept)	25	5	201	33.5	7	8	344x344x84	9.94	2.551
VESPAR (Detailed)	32.2	6.4	209.8	50.1	7.9	9.3	344x344x84	9.94	2.551
Conventional (Concept)	25	5	201	33.5	15	0	344x344x3	0.20	0.56
Conventional (Detailed)	32.2	6.4	209.8	50.1	18.4	0	391x391x3	0.237	0.66

Table 5. Generalized characteristics of radiators.

Radiator	$\Delta\overline{Q}$	$\Delta\overline{q}$	$\overline{Q}_h$	φ_h	C_M [kg/W]	C_V [l/W]
VESPAR (Concept)	0.8	0.833	0.28	0.172	0.25	1.22
VESPAR (Detailed)	0.8	0.761	0.245	0.157	0.20	1.04
Conventional (Concept)	0.8	0.833	0.6	0.368	-	-
Conventional (Detailed)	0.8	0.761	0.57	0.366	-	-

Moreover, the magnitude of the criterion of the control power need, φ_h, for VESPAR is less than half the value for the conventional radiator. This efficiency on heater power saving comes on the cost of additional mass and volume: respectively, around 0.20 kg and 1.04 liter per 1 W of heater power saved.

Conclusions

A new concept of space radiator with variable emittance was presented. Using a recently developed temperature dependent variable emissivity coating and an innovative geometry, it has no moving parts being in principle more reliable than the conventional thermal louvers.

Named VESPAR, it has its concept feasibility verified numerically through a design optimization approach, and the results demonstrated that it has a great potential to be used in applications where the electrical power available to be used by the satellite thermal control subsystem is very limited. In the presented case, VESPAR demonstrates about twice lesser requirement for the control power than a conventional radiator.

In-orbit simulation confirms that the introduced variable thermal resistance between two stages in HC is small enough to be compensated by extended external 2nd stage surface available for radiation to space, even with a certain gain: in the numerical example the maximal heat power could be increased from 25 to 32.2 W using the same footprint.

The VESPAR concept intrinsic feature of the passive self-control can also contribute to a longer surviving satellite period in the case of electric power loss, because the equipment will be better prevented from the sub-cooling than in the case of the conventional radiator.

On the other hand, the efficiency of VESPAR on saving power for the satellite thermal control subsystem comes with an estimated mass penalty of 0.20 kg per Watt saved. However, this figure can be decreased significantly with the use of new light materials, like high-conductivity carbon for the radiator structure instead of Aluminum alloy. The goal is to reach figures less than 0.08 kg/W, which is the average mass performance of the onboard power supply subsystem of modern satellites (Reeves, 1999).

It is envisioned that the utilization of such kind of radiator in micro-satellites would lead to considerable electric power savings and contribute to a longer satellite life.

Acknowledgements

The authors acknowledge the financial support provided by CNPq, *Conselho Nacional de Desenvolvimento Científico e Tecnológico*, FAPESP, *Fundação de Amparo à Pesquisa do Estado de São Paulo*, and FAPERJ, *Fundação Carlos Chagas Filho de Amparo à Pesquisa do Estado do Rio de Janeiro*.

References

Bak, P. and Sneppen, K., 1993, "Punctuated equilibrium and criticality in a simple model of evolution", *Physical Review Letters*, 71, pp. 4083-4086.

Boetcher, S. and Percus, A.G., 2001, "Optimization with extremal dynamics", *Physical Review Letters*, 86, pp. 5211-5214.

De Sousa, F.L., Ramos, F.M., Paglione, P. and Girardi, R.M., 2003, "New Stochastic Algorithm for Design Optimization", *AIAA Journal*, Vol. 41, No. 9, pp. 1808-1818.

Fleischman, G.L., Pasley, G.F., McGrath, R.J., Loudenback, L.D., 1978, "A high reliability variable conductance heat pipe space radiator". In: 3rd IHPC - International Heat Pipe Conference, Palo Alto, Calif., May 22-24, 1978, Paper A78-35576 14-34, New York, *AIAA*, pp. 216-226.

Fonseca, I.M., Arantes Júnior, G., Bainum, P.M., 2004, "On the Equars Attitude Dynamics and Control". In: International Astronautical Congress, IAC, 2004, Vancouver. 55 th IAC Final Papers. Vancouver: ZARM, 2004. v. CD I. pp. 1-11.

Gilmore, D.G., 2002, "Spacecraft Thermal Control Handbook", Volume 1: Fundamental Technologies. The Aerospace Corporation Press, California, United States.

Isachenko, V.P. and Sukomel, A.S.A., 2000, "Heat Transfer", ISBN: 089875027X, International Law & Taxation

Karan, R.D., 1998, "Satellite Thermal Control for Systems Engineers", Vol. 181, Progress in Astronautics and Aeronautics, 286 p.

Kono, J., Quintino, M., Rudorff, B. and Carvalho, H., 2003, "The Amazon Rainforest Monitoring Satellite – SSR-1". Acta Astronautica, 52, pp. 701-708.

Lino, C.O., Lima, M.G.R., Hubscher, G.L. CBERS - An International Space Cooperation Program. Acta Astronaurica, Vol. 47, Nos. 2-9. pp. 559-564.

Messac, A., Sundararaj, G.J., Tappeta, R.V. and Renaud, J.E., 2000, "Ability of Objetive Functions to Generate Points on Nonconvex Pareto Frontiers", *AIAA Journal*, Vol. 38, No. 6, pp. 1084-1091.

Muraoka, I., De Sousa, F.L., Parisotto, W.R. and Ramos, F.M., 2001, "Numerical and Experimental Investigation of Thermal Louvers for Space Applications", *Journal of the Brazilian Society of Mechanical Sciences*, Vol. XXIII, No. 2, pp. 147-153.

Panczak, T.D., Ring, S.G., Welch, M.J., Johnson, D., 2005, "Thermal Desktop® A CAD Based System for Thermal Analysis and Design 4.8 Version, User's Manual". Cullimore and Ring Technologies, Inc. (www.crtech.com), 783 p.

Parisotto, W.R., Muraoka, I. and Ramos, F.M., 1996, "Analysis and Development of Thermal Louvers for the Brazilian Space Program", 20th International Symposium on Space Technology and Science, Gifu, Japan, May 19-25.

Reeves, E.I., 1999, "Spacecraft Design and Sizing", Space Mission Analysis and Design, James R. Wertz, Wiley J. Larson, Editors, Microcosm Press and Kluwer Academic Publishers, pp. 301-352.

Shimakawa, Y. et al., 2002, "A variable-emittance radiator based on a metal-insulator transition of (La,Sr)MnO3 thin films", *Applied Physics Letters*, 80, pp. 4864-4866.

Tachikawa S. et al., 2000, "Design and Ground Test Results of a Variable Emittance Radiator", Proceeding of the 30th ICES – International Conference on Environmental Systems, Toulouse, France, July, Paper SAE 2000-01-2277.

Tachikawa S., Ohnishi A., Shimakawa Y., Ochi A., Okamoto A. and Nakamura Y., 2003, "Development of Variable Emittance Radiator Based on a Perovskite Magnese Oxide", *Journal of Thermophysics and Heat Transfer*, Vol. 17, No. 2, April-June 2003, pp. 264-268.

Tachikawa S., Ohnish A., Shimazaki K., Okamoto A., Nakamura Y., Shimakawa Y., Mori T. and Ochi A., 2001, "Smart Radiation Device: Design of an Intelligent Material with Variable Emittance", Proceeding of the 31th ICES – International Conference on Environmental Systems, World Resort, Orlando, USA; July 9-12, Paper SAE 2001-01-2342, pp. 1-5.

Vanderplaats, G.N., 1998, "Numerical Optimization Techniques for Engineering Design", Vanderplaats Research & Development, Inc., Colorado Springs, United States, 417 p.

Vlassov, V.V., De Sousa, F.L. and Takahashi, W.K., 2006a, "Comprehensive Optimization of a Heat Pipe Radiator Assembly filled with Ammonia or Acetone", *International Journal of Heat and Mass Transfer*, Vol. 49, Issues 23-24, pp. 4584-4595.

Vlassov, V.V., Cuco, A.P.C., De Sousa, F.L., Silva Neto, A.J.S., 2006b, "Design optimization of two-stage radiator with variable emittance: analysis of concept feasibility". Proceeding of 11th Brazilian Congress of Thermal Engineering and Sciences – ENCIT2006, December 5-8, 2006, Curitiba, Paraná, Brazil.